Solid State Communications, Vol. 77, No. 1, pp. 33-38, 1991.
Printed in Great Britain.

0038-1098/91$3.00+.00
Pergamon Press plc

Three-Dimensionally Confined Diluted Magnetic Semiconductor Clusters: $Zn_{1-x}Mn_xS$

Ying Wang and Norman Herron
Central Research and Development Department, E. I. DuPont de Nemours & Co., P. O. Box 80356
Wilmington, DE 19880-0356
contribution no. 5469

Karin Moller and Thomas Bein
Department of Chemistry, University of New Mexico, Albuquerque, NM 87131

(Received 23 August 1990 by J. Tauc)

We report the first example of a dilute magnetic semiconductor (DMS) confined in all three dimensions (DMS quantum dot). $Zn_{0.93}Mn_{0.07}S$ clusters of ~25 Å diameter are successfully synthesized inside a glass matrix and fully characterized by chemical analysis, x-ray diffraction, extended x-ray absorption fine structure (EXAFS), and photoluminescence spectroscopy. Effect of size quantization on the exciton energy has been observed. Preliminary magnetic susceptibility data are presented and discussed.

Diluted magnetic semiconductors (DMS) of the type $A^{II}_{1-x}Mn_xB^{VI}$, where a part of the Group II cation, A, is randomly substituted by the magnetic ion, Mn^{++}, have received extensive studies recently.[1] The presence of localized magnetic ions in a semiconductor alloy leads to an exchange interaction between the sp band electrons and the d electrons of the Mn^{++}. This sp-d exchange interaction constitutes a unique interplay between semiconductor physics and magnetism and results in unusual magneto-transport and magneto-optic phenomena such as a large Faraday rotation, giant negative magneto-resistance, and a magnetic-field-induced metal-insulator transition.[1] Their ternary nature also makes it possible to tune the band parameters and lattice constants by varying the alloy composition. These latter properties makes them attractive candidates for the preparation of superlattices and multiple quantum well structures with molecular beam epitaxy. The successful preparation of superlattices and the consequent extension of the study of DMS to the two-dimensional regime represents one of the most exciting recent developments in the area of DMS and presents a whole new set of challenges and opportunities.[1-5]

In this letter we report, what we believe to be, the first successful fabrication and characterization of diluted magnetic semiconductor clusters confined in all three dimensions, i.e. DMS quantum dots. We report detailed preparation procedures and characterization by x-ray diffraction, EXAFS, and photoluminesce spectroscopy. The effects of quantum-confinement on the optical absorption spectra and the magnetic susceptibility have been observed and will be discussed. This study of DMS quantum dots represents part of our continuing program in developing synthetic methodology and fundamental understanding of semiconductor clusters.[6-7]

We chose $Zn_{1-x}Mn_xS$ as the first system for study. From the previous work on II-VI semiconductor clusters[6,7], it is known that small clusters of this type exist in the zinc blende (sphalerite) structure. This is compatible with the known zinc blende structure of $Zn_{1-x}Mn_xS$ when $x < 0.1$.[8] Similar considerations also suggest that $Cd_{1-x}Mn_xS$ is not a good candidate, at least initially, since it exists in the wurtzite structure for x up to ~0.45, and therefore not

compatible with the zinc blende structure preferred by small clusters. The matrix chosen to support the DMS clusters is silicate glass prepared by the sol-gel method. With this method, the pore size of the sol-gel glass, and therefore the cluster size, can be easily controlled. The detailed fabrication procedure is now given below.

The first step is to include Zn^{2+} and Mn^{2+} cations into the initial sol . 5ml tetramethylorthosilicate was mixed with 8.33ccs methanol in a 25ml flask. A second solution consisting of 0.67ccs nitric acid, 6ccs water, 0.01g manganese nitrate and 0.33g zinc nitrate (the Mn doping level is controlled by varying this ratio of Zn/Mn nitrates in this original solution) was prepared and added to the first with vigorous stirring. After 5minutes the solution was cast into 6 polypropylene vials (2cm diameter, solution 5mm deep) and tightly capped. After standing at room temperature overnight, the solution had set to a rigid gel which was dried by uncapping the vials and flushing with air in a convection oven at 60°C for 24 hours. The glass disks shrunk to approximately half their original size during this operation. The final stages of drying/calcination were done in flowing (10cc/min) oxygen with a temperature ramp from 25°C to 250°C over 24 hours. At this stage the dried porous glass disks are about 1/3 their original size and very absorbent and so must be protected from atmospheric moisture and other contaminants. Due to partial oxidation of the included manganese during the oxygen calcination step, the glass typically has a light pink/purple coloration at this stage.

To generate the $Zn_{1-x}Mn_xS$ clusters, the Zn^{2+} and Mn^{2+}-containing glass disks were exposed to hydrogen sulfide on a vacuum line by evacuation at 200°C followed by introduction of 500 torr H_2S. After heating at 200°C for 30mins the sample was evacuated and re-pressured with fresh hydrogen sulfide for a further 30mins at 200°C. Finally the disks were cooled to room temperature in high vacuum. For optical measurements, the disks were transported into an inert atmosphere dry box and there impregnated with a 1% solution of Vazo-64 radical initiator in methylmethacrylate. Following gentle heating to 60°C overnight the acrylate polmerized throughout the glass generating a dense glass/polymer composite with no residual porosity. This composite is strong enough to allow traditional cutting and polishing to give thin clear disks (~1mm thick) suitable for spectroscopy and with reduced light scattering [9]. The stochiometry of the composition is established by chemical analyses (Galbraith, TN).

The sample prepared for the present study has the formula $Zn_{0.93}Mn_{0.07}S$ with a slight excess of Zn and Mn (9.6×10^{-4} mole/100g glass). The concentration of the $Zn_{1-x}Mn_xS$ cluster in glass is 4.56 wt%. X-ray diffraction pattern (with CuKα radiation, λ=1.541 Å) shows weak but distinct peaks at 2θ of 28.7°, 47.5°, and 56.5°, corresponding to the (111), (220), and (311) planes, respectively. These values are essentially the same as those of bulk, sphalerite ZnS, and indicate there is not much change in the lattice constant of ~25 Å $Zn_{0.93}Mn_{0.07}S$ clusters from that of ZnS. For bulk $Zn_{1-x}Mn_xS$, the lattice constant increases by about 0.2% from ZnS to $Zn_{0.93}Mn_{0.07}S$.[10] This increase can be easily offset by the decrease in lattice constant sometimes observed for small II-VI clusters.[7] From the width of the x-ray diffraction peaks, we calculate the size of the cluster using the Scherr's equation: $D=k\ell/\beta\cos\theta$, where k is a shape factor taken to be 1, D is the diameter, ℓ is the x-ray wavelength (1.541 Å), θ is the diffraction angle and ß is the angular half-width of the diffraction peak in 2θ. Based on a direct computer simulation study,[11] this Scherr's equation underestimates the diameter of a spherical cluster by about 15% and is corrected for here. The sample used in this study contains $Zn_{1-x}Mn_xS$ clusters with an averaged diameter of ~25Å (±20%). Clusters of this size contain approximately 160 Zn, 10 Mn, and 170 S atoms.

EXAFS was used to probe the local enviroment of the Mn^{2+}dopant. The data were taken at the National Synchrotron Light Source in Brookhaven National Laboratories with a stored electron energy of 2.5 GeV and ring currents between 80-120 mA on beamline X11A. Measurements were performed in transmission with a Si(111) crystal pair on the Mn absorption-edge (6539 eV) at liquid nitrogen temperature. Standard procedures[12] for data analysis were followed. Figure 1 compares Fourier transformed EXAFS data of the sample before and after H_2S treatment. EXAFS analysis of the Zn^{2+} and

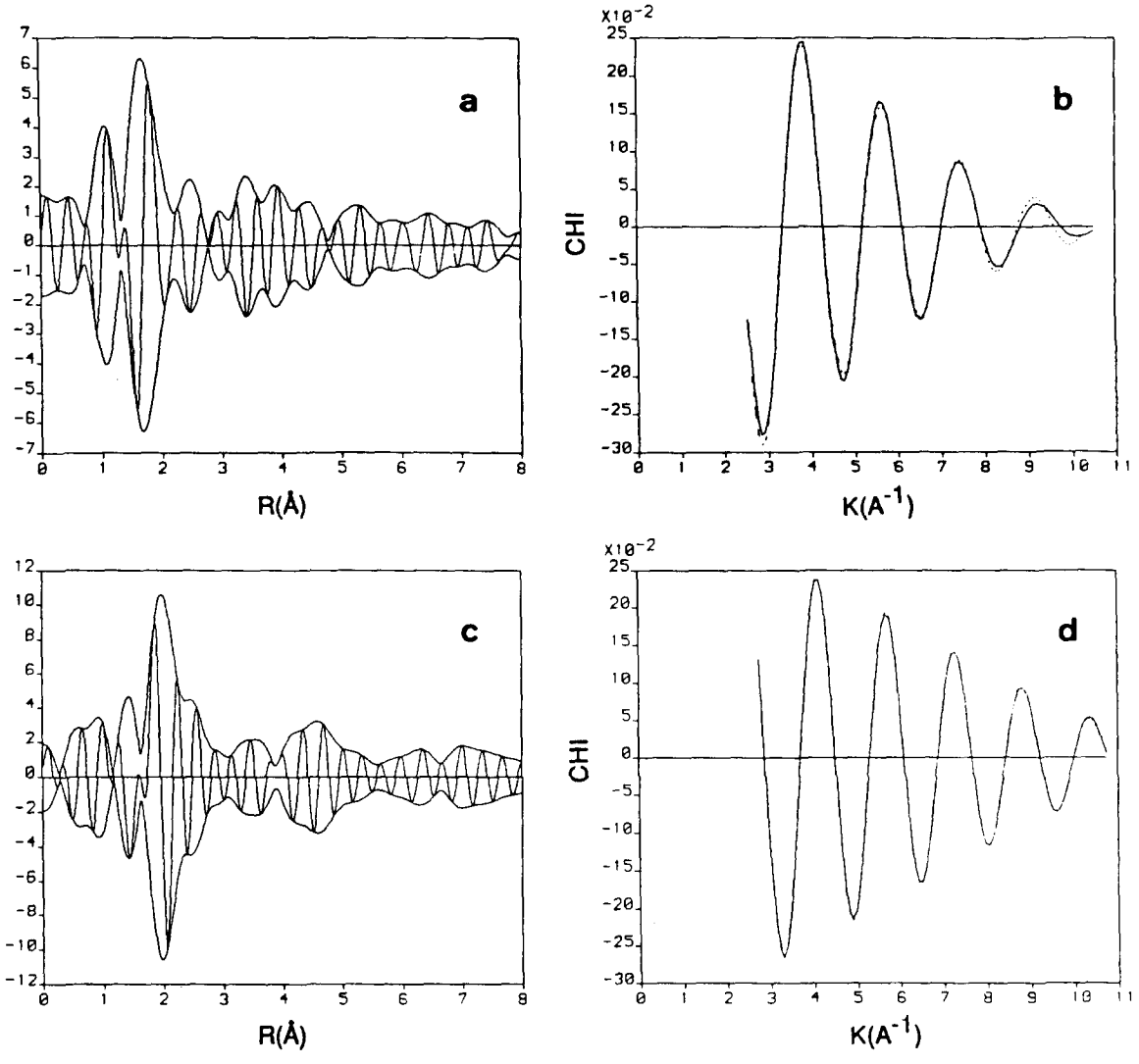

Figure 1. K^3 weighted Fourier transformations of the sample before (1a) and after H_2S treatment (1c) and corresponding backtransformations of the first coordination spheres (solid line) and fits (broken line).

Mn^{2+}-containing glass (before H_2S treatment, Figure 1a) shows that Mn is surrounded by six oxygen atoms with a bond distance typical for bulk MnO (2.19Å). The corresponding fit of the first neighbor shell is shown in Figure 1b. Upon H_2S exposure, the coordination sphere of Mn has changed from oxygen to sulfur as indicated by the phase change of the imaginary part in the Fourier transform (Figure 1c). Mn-S is formed with a bond length of 2.45 Å and a coordination number of 4.6 (Figure 1d). This Mn-S bond length is slightly longer than the Zn-S bond length, 2.35 Å. This trend is consistent with the results of a previous EXAFS study[13] of bulk $Zn_{1-x}Mn_xSe$, which yields a Zn-Se bond length of 2.45 Å and a Mn-Se bond length of 2.55 Å in the whole composition range of $0<x<0.55$. The measured Mn-Se bond length is essentially the hypothetical zinc blende Mn-Se bond length obtained by extrapolation with Vegard's law.[1] The EXAFS results therefore support the notion that Zn^{2+} is randomly

substituted by Mn^{2+} in the ~25 Å $Zn_{0.93}Mn_{0.07}S$ clusters and the Mn^{2+} ions are located inside the clusters.

Photoluminescence and excitation spectra of ~25 Å $Zn_{0.93}Mn_{0.07}S$ clusters are shown in Figure 2a. The relatively sharp emission band at 594 nm is due to Mn^{2+} in $Zn_{1-x}Mn_xS$.[14] The weak shoulder at ~700 nm comes from defect states, the origin of which is unknown at present. As shown in Figure 2a, the intensity of the defect emission can be reduced by annealing the sample at room temperature. The temperature dependence of the Mn^{2+} luminescence intensity is shown in Figure 2b. The luminescence intensity stays relatively constant below 50 K and then drops quickly above ~50 K. This temperature dependence can be modeled by the multiphonon induced radiationless transition theory,[15] which describes the nonradiative relaxation of an excited state stimulated by the excitation and emission of the mediating phonons. Qualitatively the frequency of the mediating phonons determines the starting thermal quenching temperature. A quantitative analysis was performed on these

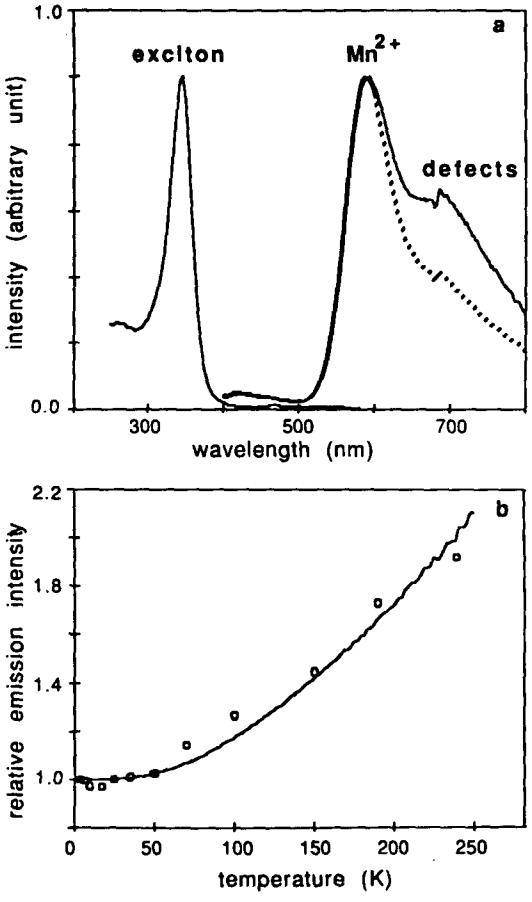

Figure 2. (a) The normalized excitation and luminescence spectra of ~25 Å $Zn_{0.93}Mn_{0.07}S$ clusters in glass at room temperature. The exciton peak in the excitation spectrum is located at 346 nm. The dotted curve with the reduced defect luminescence intensity was obtained several days after the upper curve was taken. (b) The relative luminescence intensity at 594 nm, I(temperature=3.7 K)/I(t), plotted as a function of the temperature. The solid curve is a theoretical fit described in the text.

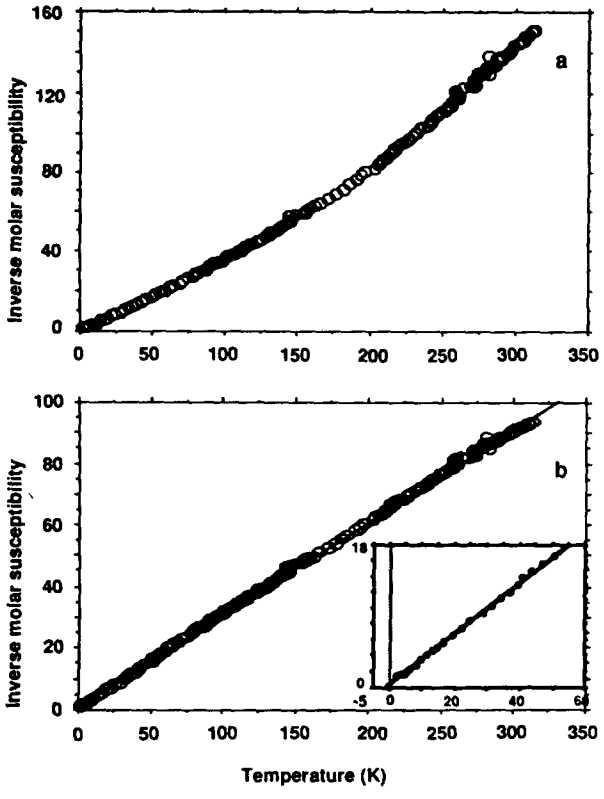

Figure 3. (a)T he inverse molar susceptibility of ~25 Å $Zn_{0.93}Mn_{0.07}S$ clusters in glass plotted as a function of the temperature. (b) The corrected inverse molar susceptibility, $1/(\chi-A)$, plotted as a function of the temperature. The solid line represents a fit to the equation $\chi = A + C/(T-\theta)$ with $A=-5.5\times10^{-3}$, C=3.69, and ,θ=-0.282. The inset shows an expanded plot in the low temperature region.

data. Our data analysis[16] and the details of the theory[15] have been presented before and will not be repeated here. In Figure 2b, the solid line is the theoretical fit based on equations (1) to (10) in reference 16. For the Mn^{2+} luminescence, the data can be fitted with an effective mediating phonon frequency of 101 cm^{-1} and a Franck-Condon displacement factor of 122, which yields a coupling parameter S ~ 1.4 (intermediate-coupling regime). In the weak-coupling limit (S>1), the effective phonon frequency is close to the highest phonon frequency in the medium. In the intermediate-coupling regime (S~1), lower frequency phonons also contribute and the effective phonon frequency represents an "average" of all contributing phonons. For ZnS, the highest phonon frequency is ~300 cm^{-1}. The measured effective phonon frequency of ~100 cm^{-1} therefore confirms the idea that a majority of the Mn^{2+} ions are substitutionally distributed within the ZnS lattice of the cluster. Otherwise, Mn^{2+} would be coupled to much higher frequency phonons, if they are mostly located on the surface or outside the cluster, due to the presence of higher frequency Si-O bonds in the matrix such as we have found previously in other systems.[16]

In the excitation spectrum a sharp ZnS exciton peak at 346 nm is observed (Figure 2a). Bulk $Zn_{1-x}Mn_xS$ of the same composition shows an exciton peak at 370 nm in the excitation spectrum. This blue shift in the band gap from 370 to 346 nm (0.23 eV) is a direct result of the quantum confinement effects.[6,7,17-21] The simple three-dimensional confinement model based on effective mass approximation predicts the energy shift, ΔE, as[17-19]

$$\Delta E = \frac{\hbar^2 \pi^2}{2R^2}\left[\frac{1}{m_e}+\frac{1}{m_h}\right] - \frac{1.786\, e^2}{\varepsilon R} - 0.248\, E^*_{Ry} \quad (1)$$

where R is cluster radius, m_e is the electron effective mass, m_h is the hole effective mass, ε is the dielectric constant, and E^*_{Ry} is the effective Rydberg energy, $e^4/2\varepsilon^2\hbar^2(m_e^{-1} + m_h^{-1})$. The first term in eq. (1) represents the kinetic energy, the second term the Coulomb energy, and the third term is a result of the correlation effect.[19] For a 25 Å ZnS cluster, we calculate ΔE to be 0.65 eV, using m_e=0.34, m_h=0.58, and ε=5.13.[22] For a 30Å ZnS cluster the calculated shift is 0.42 eV. Compared to the experimentally observed value of 0.23 eV, the calculation overestimates the shift in band gap produced by the quantum confinement effect. This discrepancy between the simple theory and experiments has also been observed for other small semiconductor clusters.[7,20-21,23] In the case of PbS,[20] the breakdown of the effective mass approximation is clearly the major reason for the failure of the simple model represented by eq.(1).

The Mn-Mn interaction represents one of the most interesting topics in the field of DMS. For bulk DMS the Mn-Mn interaction is antiferromagnetic and there exists two different magnetic phases, depending on the Mn concentrations and the temperature. The phase diagram consists of a high-temperature paramagnetic phase and a low-temperature frozen phase (often called a spin-glass phase). The transition to the spin-glass-like phase is manifested as a "cusp" in the temperature-dependent magnetic susceptibility data. Based on an empirical picture of magnetic freezing,[1] it was suggested that the aggregation or the "networking" of small antiferromagnetically ordered clusters (or domains) is the main reason leading to the formation of spin-glass-like phase. When the dimensionality of DMS is reduced as in the case of $Cd_{1-x}Mn_xTe$ superlattice, it was found[5] that the cusp in the susceptibility disappeared for superlattices with thickness ≤20 Å, indicating the inability of the two-dimensional systems to support long-range spin-glass order. It was further suggested[1] that this may be an indication of the suppression of antiferromagnetic order within the cluster. From this viewpoint, it is of considerable interest to study the magnetic susceptibility of DMS quantum dots.

Figure 3a shows the static magnetic susceptibility data (×) of ~25 Å $Zn_{0.93}Mn_{0.07}S$ plotted as 1/× vs. temperature from 314 to 2.3 K. There is a curvature in the plot at higher temperatures which is most likely originated from defects in the sample, as demonstrated in the photoluminescence experiments (Figure 2a). We found that the data can be fitted to the equation $\times = A + C/(T-\theta)$, where θ is the Curie-Weiss temperature (Figure 3b). The best fit gives $A=-5.5\times10^{-3}$, C=3.69, and θ=-0.282

(Figure 3b) where A is obtained independently from the intercept of the $\times$ vs. 1/T plot in the high temperature limit (above 200 K). Alternatively, we fitted the lower temperature portion of the data (2.3 to ~80 K) with the Curie-Weiss law and obtained essentially the same information. The very small negative Curie-Weiss temperature indicates paramagnetism. The antiferromagnetic interaction between Mn ions in these clusters is either very weak or absent. This result is consistent with the idea that antiferromagnetic ordering can be suppressed in a small DMS cluster. From the Curie constant, C, we determined the effective moment to be 5.43, which can be used to check the valence state of the manganese ions. The effective moment, μ_{eff}, is defined as

$$\mu_{eff} = [\, g^2 S(S+1)]^{1/2} \mu_B \qquad (2)$$

where g is Lande factor (g=2), S is the magnetic moment, and μ_B is the Bohr magneton. For a Mn^{2+} ion, the magnetic moment is 5/2 which gives a μ_{eff} value of 5.9, in reasonable agreement with the experimental value.

To reach a definitive conclusion about the confinement effect on the magnetic properties, one needs to measure the magnetic susceptibility as a function of the cluster size, which is currently being pursued in our lab. One can also simulate the hypothetical spin-glass formation process by increasing the DMS cluster concentration above the percolation threshold. With the DMS quantum dots now synthetically available, all these and other interesting issues can be systematically examined.

Acknowledgements- We thank S. H. Harvey and J. B. Jensen for the excellent technical assistance and R. S. McLean for the magnetic susceptibility measurements.

References

1. For a recent review, see J. K. Furdyna, J. Appl. Phys. 64, R29(1988).
2. L. A. Kolodziejski, T. C. Bonsett, R. L. Gunshor, S. Datta, R. B. Bylsma, W. M. Becker, and N. Otsuka, Appl. Phys. Lett. 45,440(1984).
3. R. N. Bicknell, R. W. Yanka, N. C. Giles-Taylor, D. K. Blanks, E. L. Buckland, and J. F. Schetzina, Appl. Phys. Lett. 45, 92(1984).
4. S. Datta, J. K. Furdyna, and R. L. Gunshor, Superlattices and Microstructures 1, 317(1985).
5. D. D. Awschalom, J. M. Hong, L. L. Chang, and G. Grinstein, Phys. Rev. Lett. 59,1733(1987).
6. Y. Wang, N. Herron, W. Mahler, and A. Suna, J. Opt. Soc. Am. B 6, 808(1989).
7. N. Herron, Y. Wang, and H. Eckert, J. Am. Chem. Soc. 112,1322(1990).
8. "Landolt-Bornstein, New Series", Vol. III, subvol. 17b, edited by O.Madelung, Springer-Verlag, New York, 1983, p.528.
9. E. J. A. Pope, M. Asami, J. D. Mackenzie J.Mater.Res 4, 1018 (1989)
10. "Landolt-Bornstein, New Series", Vol.III, subvol.17b, edited by O.Madelung, Springer-Verlag, New York, 1983, p.311.
11. A. Suna and Y. Wang, unpublished results.
12. P. A. Lee, P. H. Citrin, P. Eisenberger, and B. M. Kincaid, Rev. Mod. Phys. 53, 769(1981).
13. B. A. Bunker, W.-F. Pong, V. Debska, D. R. Yoder-Short, and J. K. Furdyna, in "Diluted Magnetic (Semimagnetic) Semiconductors", edited by R. L. Aggarwal, J. K. Furdyna, and S. von Molnar (Materials Research Society, Pittsburgh, PA, 1987), Vol.89, p.231.
14. D. Langer and S. Ibuki, Phys. Rev. 138, A809(1965).
15. F. K. Fong, "Theory of Molecular Relaxation. Applications in Chemistry and Biology", Wiley, New York, 1975.
16. Y. Wang and N. Herron, J. Phys. Chem. **92**,4988 (1988).
17. AI. L. Efros and A. L. Efros, Sov. Phys. Semicond. **16**, 772 (1982).
18. L. E. Brus, J. Chem. Phys. **80**, 4403(1984).
19. Y. Kayanuma, Phys. Rev. B 38,9797(1988).
20. Y. Wang, A. Suna, W. Mahler, and R. Kasowski, J. Chem. Phys. **87**,7315, (1987).
21. A. Henglein, Topics in Current Chemistry, **143**,113(1988).
22. "Landolt-Bornstein, New Series", Vol. III, subvol.17b, edited by O.Madelung, Springer-Verlag, New York, 1983, p. 61.
23. P. E. Lippens and M. Lannoo, Phys. Rev. B 39, 10935(1989).